

Unusual Li-Storage Behaviour of Two-Dimensional ReS₂ Single Crystals

Apoorva Chaturvedi,^[a] Peng Hu,^[a] Ayan Ray,^[c] Christian Kloc,^[a] Srinivasan Madhavi,*^[a] and Vanchiappan Aravindan*^[b]

Unusual Li-storage properties are observed for two-dimensional ReS₂ compared to its analogue MoS₂. First, we prepared ReS₂ single crystals (99.9% crystallinity) by chemical vapour transport with high yield and utmost purity. Li-storage properties are assessed using a standard half-cell assembly with metallic Li as the counter electrode. The highly crystalline ReS₂ rendered excellent electrochemical characteristics with interesting features. This logically leads to further exploration of ReS₂ towards

Li-storage. Indeed, ReS₂ could act as efficient intercalation host for Li-ions with lower redox potential (~1.2 V vs. Li) and decent reversibility (~0.4 mol Li). On the other hand, high reversibility is registered while deep discharging of the active material. This eventually obeys the perfect conversion pathway. Interestingly, electrochemically activated ReS₂ also rendered good reversibility and eventually serves as an insertion host with a working potential of ~2 V vs. Li.

1. Introduction

Lithium-ion batteries (LIB) continue to conquer the commercial market by powering numerous electronic gadgets, like computers, cameras, toys, and other appliances. Further, powering hybrid and electric vehicles (HEV and EV) is also explored using high energy LIBs, besides their grid storage applications.^[1–7] Generally, LIBs are composed of graphite as the negative electrode and either layered LiCoO₂, LiMn_{1/3}Ni_{1/3}Co_{1/3}O₂, or olivine phase LiFePO₄ is engaged as positive electrode.^[1,8,9] Although graphite is well established as a negative electrode, it suffered a lot during high current operation. This eventually leads to the Li-plating on the graphite surface and subsequent, dendritic growth as well. The limited capacity is another important factor (~372 mAh g⁻¹). Therefore, search for alternate anode materials is highly accelerated. Compared to graphite, spinel Li₄Ti₅O₁₂ exhibits a lower theoretical capacity (~175 mAh g⁻¹) and a higher Li-insertion potential (~1.55 V vs. Li), but is still considered and commercialized as a promising high power anode in HEV and EV applications.^[10] Several binary and ternary metal oxides (anatase and bronze phases of TiO₂, Nb₂O₅,

LiCrTiO₄ etc.,) and sulphides (TiS₂, MoS₂ etc.,) are considered as promising candidates for this category.^[8,11–13] Among these, two-dimensional (2D) di-chalcogenides with a molecular formula of MS₂ (M = Ti, Mo, Re etc.) is found appealing in terms of highly reversible intercalation properties and decent working potentials.^[13–18] Since the exploration of conversion type anodes, these 2D di-chalcogenides are also seriously investigated for extending the Li-storage capability.^[15,16,19–21] TiS₂ and MoS₂ have been investigated as promising candidates for intercalation and conversion mechanisms, respectively, while TiS₂ is also well-known and commercialized as a cathode with metallic Li in the early period of battery development.^[15,22,23] On the other hand, MoS₂ has been seriously explored as high capacity conversion anode, but due to its large polarization, huge irreversibility and poor cyclability, the potential use as an anode in practical configurations is limited.^[8,24] Although TiS₂ and MoS₂ belong to the same family of 2D layered structures, the underlying charge storage mechanisms are different. ReS₂ is another fascinating material belonging to the same family. It exhibits a theoretical capacity of ~428 mAh g⁻¹(for the conversion reaction) but from the LIB point of view, it has not been explored in detail yet.

Herein, we are investigating the Li-ion storage properties and evaluate the battery performance of ReS₂ single crystals. For the synthesis of ReS₂ single crystals of high purity, chemical vapour transport (CVT) is used, allowing the formation of nearly 100% crystalline compounds. Extensive structural and electrochemical studies are performed and discussed in detail. To investigate the Li-storage capability and its storage mechanism, three different cut-off potentials are engaged.

2. Results and Discussion

ReS₂ exhibits a layered, flat plate-like morphology as shown in Figure 1b. A representative crystal structure with different orientation has been simulated with Vesta 3.3 program to

[a] Dr. A. Chaturvedi, Dr. P. Hu, Prof. C. Kloc, Prof. S. Madhavi

School of Materials Science and Engineering

Nanyang Technological University

Singapore 639798

E-mail: Madhavi@ntu.edu.sg

[b] Dr. V. Aravindan

Department of Chemistry

Indian Institute of Science Education and Research (IISER)

Tirupati-517507, India

E-mail: aravind_van@yahoo.com

[c] Dr. A. Ray

Department of Physics

School of Engineering & Applied Science

Bennet University

Greater Noida, Uttar Pradesh, India

 Supporting Information and the ORCID identification number(s) for the author(s) of this article can be found under:

<https://doi.org/10.1002/batt.201800018>

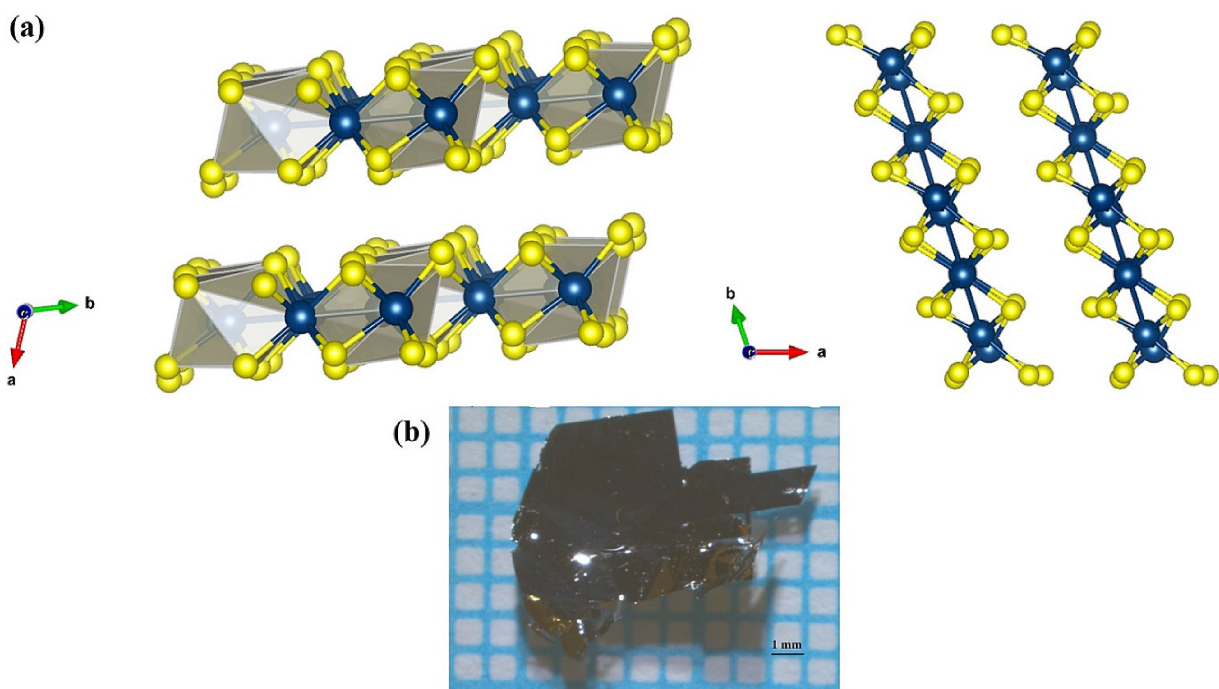


Figure 1. (a) Simulated crystal structure of ReS₂ (PDF # 00-052-0818) showing the layered morphology in different orientations. (b) Optical Image of as-grown typical ReS₂ crystal flake.

depict the atomic arrangement and most importantly availability of van der Waals spaces between chalcogen-metal-chalcogen trilayers useful for storage applications (Figure 1a). The powder X-ray diffraction (P-XRD) studies were performed on background-less sample holder such that flat, 2D bulk crystallites orientate perpendicular to the face of the sample holder. In this way, strong diffraction peaks in $(00l)$ direction were detected and the low diffraction peaks from other planes are masked as shown in Figure 2 (a). All the peaks were indexed to the PDF # 00-052-0818 revealing the high crystallinity and phase purity.^[25] In addition, SEM/EDAX measurements were performed to assess the semi-quantitative data of the prepared compound. The data shown in Figure 2b confirmed ratio of the as-grown sample to be used for Li-storage measurements.

The detailed atomic arrangement of ReS₂ crystals was investigated using High-Resolution Transmission Electron Microscopy (HR-TEM). A crystalline flake is visible from the low-resolution TEM image with sharp edges meeting at around 120° angle consistent with characteristic distorted hexagonal structure of ReS₂ and corresponding higher resolution by keeping the area of interest near the sharp edges meeting at the corner (Figure 2c). A select area electron diffraction (SAED) pattern was also obtained for the same crystalline flake as shown in Figure 2d with the scanned area earmarked by a black circle. The atomic arrangement indicates triclinic symmetry or distorted CdI₂ structure consistent with the previous reports.^[26] X-ray photoelectron spectroscopic studies also performed to validate the composition of ReS₂ single crystals prepared, and the studies are in good agreement with the analysis described above (Figure S1).

Li-storage properties of the CVT derived ReS₂ is investigated in half-cell assembly for a wide potential range between 0.005 to 3 V vs. Li at a current density of 50 mA g⁻¹ and given in Figure 3. Apparently, a prominent plateau is noted at ~ 1.2 V vs. Li with corresponds to the intercalation of ~ 0.74 mol of Li ($\text{ReS}_2 + 0.74 \text{ Li} + 0.74 \text{ e}^- \rightarrow \text{Li}_{0.74}\text{ReS}_2$) followed by a long distinct discharge curve. The long distinct curve is associated with the structural destruction of lithiated phase ($\text{Li}_{0.74}\text{ReS}_2$) and subsequent reduction into Re⁰ as fine metallic nano-particles in an amorphous Li₂S matrix ($\text{Li}_{0.74}\text{ReS}_2 + 3.26 \text{ Li} + 3.26 \text{ e}^- \rightarrow \text{Re}^0 + 2\text{Li}_2\text{S}$). This reaction is consistent with the MoS₂ analogue.^[24] In addition, the reduction of electrolyte solution also occurred in the same potential region and it cannot be ruled out for the extended plateau. This decomposition of the electrolyte certainly leads to the formation of inorganic by-products and oligomeric films in the form of solid electrolyte interphase (SEI).^[8,27] It is well known that the SEI formation consumes more amount of Li in an irreversible manner. As a result, the Li/ReS₂ cell delivered a discharge capacity of ~ 927 mAh g⁻¹. On the other hand, the capacity of ~ 591 mAh g⁻¹ only reversible ($\sim 64\%$) which is mainly because of the irreversible consumption of Li during the reduction of both active materials and electrolyte solution. As usual, upon charge process, the reduced metallic Re⁰ is oxidized to form a native ReS₂ compound based on the conversion process ($\text{Re}^0 + \text{Li}_2\text{S} \rightarrow \text{ReS}_2$) reported by Poizot et al.^[28] for metal oxides and Hwang et al.^[29] for MoS₂. In a second cycle, a completely different charge-discharge capacity profile is noted compared to the first cycle. In particular, the Li-intercalation reaction observed at ~ 1.2 V vs. Li in the first cycle is shifted towards higher potential of ~ 2 V vs. Li and beyond this potential, a conversion reaction results. However, there is

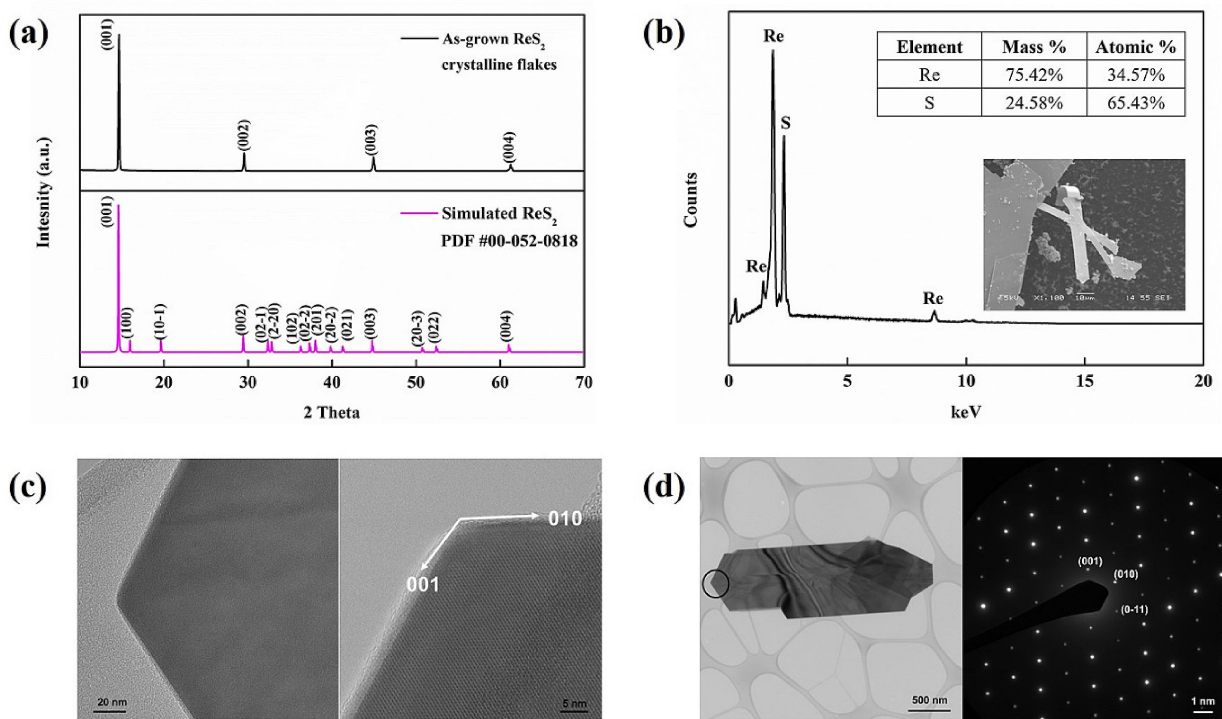


Figure 2. Materials Characterization of ReS₂ (a) Powder XRD pattern of as-grown ReS₂ compound indexed with standard PDF # 00-052-0818 (b) semi-quantitative analysis of as-grown ReS₂ crystallites. (c) High Resolution Transmission Electron Microscopy (HRTEM) images at low and high resolution (d) crystallite image with corresponding select area electron diffraction pattern (SAED). HRTEM was performed on ultra-sonicated ReS₂ sample diluted in ethanol solution.

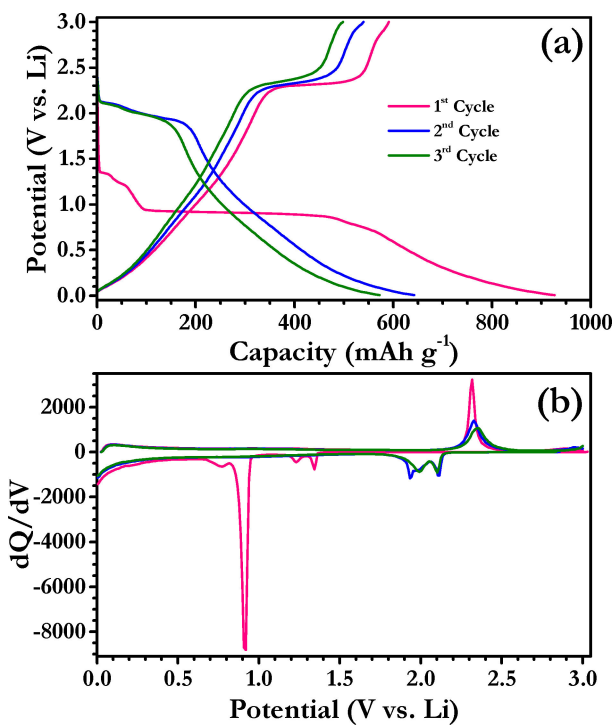


Figure 3. (a) Galvanostatic charge-discharge studies of Li/ReS₂ between 0.005 and 3 V at a current density of 50 mA g⁻¹, and (b) differential capacity profiles derived from (a). Active material loading: 10 mg.

not much deviation from the charging behaviour recorded except the intensity of the peak current. The same trend is repeated in the subsequent cycles. The differential capacity profiles of the first three charge-discharge curves are given in Figure 3b. This clearly reflects and parallels the mentioned mechanism stated above and in particular, the shift of the redox potentials. This interesting Li-storage behaviour logically led us to study the further insights in detail.

A duplicate cell was made to study the Li-insertion properties of the ReS₂ further with different cut-off potentials. A prominent Li-insertion into ReS₂ is occurred at ~1.2 V vs. Li in the first cycle and shifted to ~2 V vs. Li from second cycle onwards when the cell is cycled for a wide testing potential. In this line, we limited the lower cut-off potential to 1.05 V vs. Li instead of 5 mV vs. Li. Similarly, upper cut-off potential is adjusted to 2.7 V vs. Li and given in Figure 4. As noted above, the Li-intercalation up to ~0.74 moles is registered ($\text{ReS}_2 + 0.74 \text{ Li} + 0.74 \text{ e}^- \rightarrow \text{Li}_{0.74}\text{ReS}_2$) and the lithiated phase is consistent with wide testing window (as discussed for Figure 3). However, ~0.39 moles of Li only reversible upon subsequent charge process which corresponds to the retention of ~53% capacity which is quite lower than the wider testing range. Moreover, the partial reversibility of the lithiated phase is quite common for electrode materials, which means the residual Li has been consumed for the structural re-arrangement or irreversible phase formation. This is evident from the suppression of the predominant insertion peak of located ~1.33 V vs. Li. In the subsequent cycles, no shifting in the redox potential towards

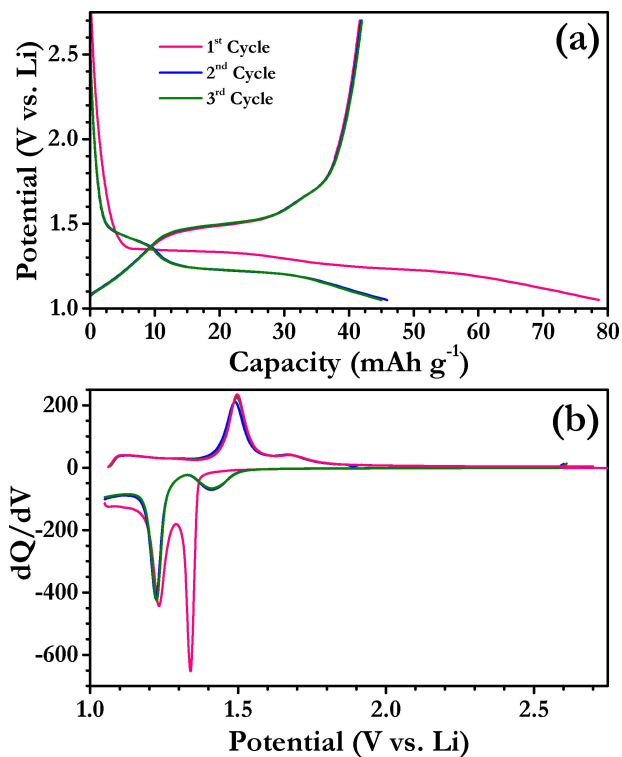


Figure 4. (a) Galvanostatic charge-discharge studies of Li/ReS₂ between 1.05 and 2.7 V at a current density of 50 mA g⁻¹, and (b) differential capacity profiles derived from (a). Active material loading: 10 mg.

higher region is observed. This behaviour is completely contradicting with its analogue MoS₂, in which such limiting testing also allows the potential to shift in higher range for redox reaction.^[30] It is clearly inferred that the ReS₂ acts as a perfect intercalation host for the insertion of Li-ions without much deviation from neither a redox potential nor a reversible capacity. The said redox reaction is clearly evident from the differential capacity profiles of charge-discharge curves (Figure 4b). We believe that the crystal structure remains intact compared to MoS₂ and ensures the stability of the host matrix. In addition, the reported works on the ReS₂ for Li-ion battery anode perspective, does not have this feature, because of the either usage of wet chemical methods used for the preparation of the active material or reported with carbonaceous composites.^[31–33] Further studies are in progress to study in depth using various analytical tools like XANES, XAFS, etc., since this report is purely based on the electrochemical aspect.

Another duplicate cell was fabricated and studied at different cut-off potentials, for example the Li/ReS₂ is cycled for a wide testing potential for first cycle (say electrochemical activation) and subsequent cycles are limited to 1.4–2.7 V vs. Li range and given in Figure 5. The Li/ReS₂ cell delivered a capacity of ~934 and ~584 mAh g⁻¹ for discharge and charge, respectively. The observed values are in line with the previous measurements and ensures the reproducibility according to the conversion mechanism stated above, $\text{ReS}_2 + 4\text{Li}^+ + 4e^- \leftrightarrow \text{Re}^0 + 2\text{Li}_2\text{S}$.^[31,32,34] From the second cycle onwards the Li/ReS₂ cell is limited to 1.4–2.7 V vs. Li with same applied current density of

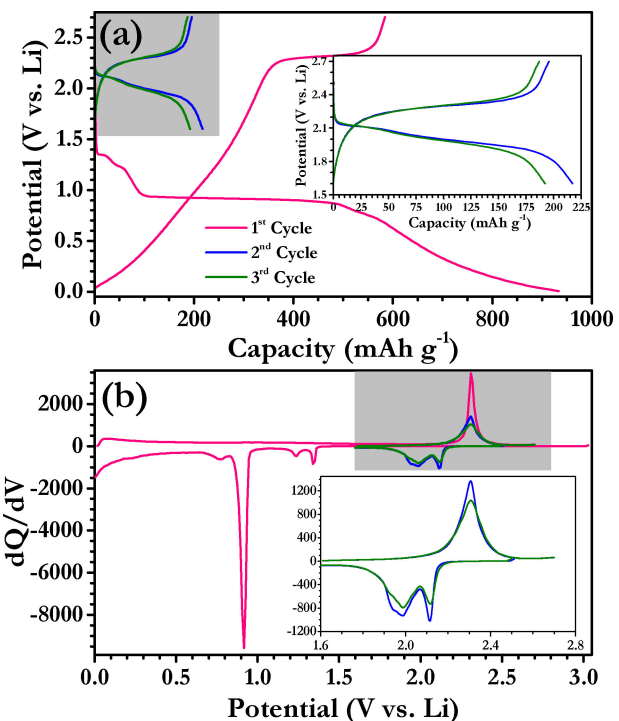


Figure 5. (a) Galvanostatic charge-discharge studies of Li/ReS₂ between 0.005 to 2.7 V for first cycle and 1.4 to 2.7 V for subsequent cycles at current density of 50 mA g⁻¹. Inset showed the charge-discharge curves from 2nd cycle onwards, and (b) differential capacity profiles derived from (a). Active material loading: 10 mg.

50 mA g⁻¹. As expected, the potential shift from the ~1.2 to ~2.1 V vs. Li is noted. However, the high reversibility is registered for example, the capacity of ~217 and ~196 mAh g⁻¹ is noted compared to the limited cycling (1.05–3 V vs. Li) as discharge and charge, respectively. An interesting fact is that the electrochemically re-formed ReS₂ delivered excellent cyclability which is consistent with its analogue MoS₂.^[24] Further, there is no diminishing in the peak intensities observed compared to restricted potential range between 1.05 to 2.7 V vs. Li range.

Cycling is one of the important aspects of electrode materials and associated energy systems as well. In this regard, the electrochemical activity of ReS₂ in half-cell assembly is evaluated for 80 cycles at current density of 50 mA g⁻¹ and given in Figure 6. The Li/ReS₂ tested at 1.05 to 2.7 V vs. Li window rendered the excellent capacity retention characteristics, which retains ~88% initial reversible capacity, whereas ~51 and ~48% (calculated from the second cycle) only retained for the cell tested at the window of 0.005 to 3 V vs. Li and multiple regions, respectively. On the other hand, the Coulombic efficiency in the 0.005 to 3 V vs. Li region exhibits slightly inferior values (>96%) whereas better values are obtained for the other two cases (>98.5%). Overall, the ReS₂ could be used as efficient anode for LIB applications at ~1.2 V vs. Li by considering the excellent cycling stability and high reversibility. However, the low capacity (<50 mAh g⁻¹) remains to be a major issue. Although, other two regions have a high capacity and rendered decent cycling profile, potential application

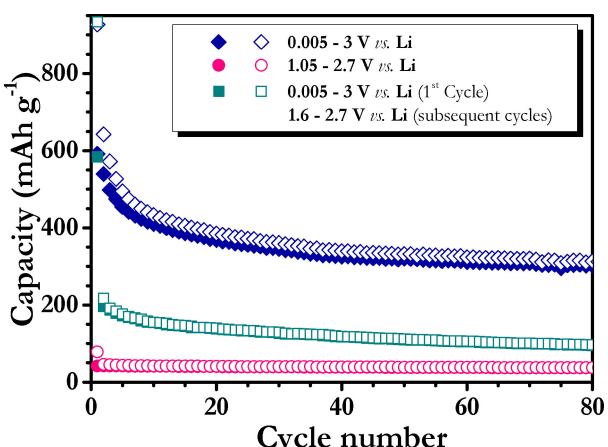


Figure 6. Cycling profiles of Li/ReS₂ cells at different cut-off potentials at a current density of 50 mA g⁻¹. The filled and open symbols correspond to the charge (filled) and discharge (open).

towards reality is handicapped by its huge polarization and wider testing window. The later issues cannot be overcome owing to the inherent property of the material. However, it will be useful i.e. pre-lithiated state will be used as efficient electrode for the fabrication of high energy Li-ion capacitors. Therefore, this preliminary half-cell studies certainly opened the avenues for the exploration of ReS₂ into potential application as negative electrode for Li-based charge storage devices like LIB and Li-ion capacitors.

3. Conclusion

We attempted to study the unique behaviour of the two-dimensional ReS₂ as a prospective anode for Li-ion battery perspective. Although, ReS₂ belongs to the family of 2D structured material with appropriate interlayer spacing (0.614 nm) like TiS₂ and MoS₂, the electrochemical activity is completely different. TiS₂ and MoS₂ are well-known electro-active materials for the sustained Li-storage in intercalation and conversion pathways, respectively. However, ReS₂ composed of both features regardless of the storage capability. This paper purely based on the electrochemical study certainly opens the further exploration of this active material for Li-ion batteries. On the other hand, the cost is one of the prime issues for this fascinating material, but there is absolutely no barrier to the fundamental research.

Experimental Section

Rhenium powder (Alfa Aesar, ~22 mesh, 99.999%, Puratronic®) and sulfur pieces (Alfa Aesar, 99.999%, Puratronic®) were used for the synthesis of rhenium disulfide (ReS₂) and subsequent crystal growth. Stoichiometric amounts of rhenium, sulfur and/or selenium were sealed in quartz ampoules with an internal pressure in the range of 10⁻⁵ to 10⁻⁶ torr. In addition to the elemental constituents, iodine (2 mg/cc) was also incorporated into the tube as a transport agent. The sealed tubes were then subjected to two-zone

horizontal tube furnace. Initially, the source zone was kept at 900 °C and the growth zone at 1000 °C for 120 hours. After this, the temperature of Zone I was gradually increased to 1060 °C while the growth zone remains at 1000 °C. This arrangement continued for next 360 hours^[25]. Further, the temperature of both the zones was lowered to room temperature and ampoules were taken out to obtain the product for characterization and measurements. The electrodes were prepared by mixing 10 mg active material (ReS₂), 1.5 mg Super P and 1.5 mg teflonized acetylene black (TAB-2) with ethanol. The slurry was placed 16 mm dia. stainless steel mesh (Goodfellow, UK) and dried in vacuum oven for overnight. CR 2016 coin-cells were used to study the Li-storage properties. Test cells were constructed with metallic Li as the counter and reference electrode separated by 19 mm Whatman paper (Cat. No. 1825-047). 1 M LiPF₆ in ethylene carbonate: di-methyl carbonate (1:1 vol.%) was used as an electrolyte. Galvanostatic studies were performed using Arbin BT 2000 in ambient temperature conditions.

Acknowledgements

This work was financially supported by National Research Foundation of Singapore (NRF) Investigatorship award number: NRF2016NRF-NRFI001-22. We would like to acknowledge the Facility for Analysis, Characterization, Testing and Simulation, Nanyang Technological University, Singapore, for use of their electron microscopy, X-ray diffraction and X-ray photoelectron spectroscopy facilities. VA thank the financial support from Science & Engineering Research Board (SERB), a statutory body of the Department of Science & Technology, Govt. of India through Ramanujan Fellowship (SB/S2/RJN-088/2016).

Conflict of Interest

The authors declare no conflict of interest.

Keywords: conversion • electrochemistry • intercalations • lithium-ion batteries • rhenium disulfide

- [1] D. Andre, S.-J. Kim, P. Lamp, S. F. Lux, F. Maglia, O. Paschos, B. Stiaszny, *J. Mater. Chem. A* **2015**, *3*, 6709–6732.
- [2] E. J. Cairns, P. Albertus, *Ann. Rev. Chem. Biomol. Engineering* **2010**, *1*, 299–320.
- [3] G. L. Soloveichik, *Annu. Rev. Chem. Biomol. Eng.* **2011**, *2*, 503–527.
- [4] H. Jiari, L. Liu, C. Yuanfu, M. Arumugam, *Adv. Mater.* **2017**, *29*, 1702707.
- [5] J. He, W. Lv, Y. Chen, K. Wen, C. Xu, W. Zhang, Y. Li, W. Qin, W. He, *ACS Nano* **2017**, *11*, 8144–8152.
- [6] J. He, Y. Chen, W. Lv, K. Wen, Z. Wang, W. Zhang, Y. Li, W. Qin, W. He, *ACS Nano* **2016**, *10*, 8837–8842.
- [7] V. Aravindan, P. Sennu, Y.-S. Lee, S. Madhavi, *J. Phys. Chem. Lett.* **2017**, *8*, 4031–4037.
- [8] V. Aravindan, Y.-S. Lee, S. Madhavi, *Adv. Energy Mater.* **2015**, *5*, 1402225.
- [9] V. Aravindan, J. Gnanaraj, Y.-S. Lee, S. Madhavi, *J. Mater. Chem. A* **2013**, *1*, 3518–3539.
- [10] M. M. Thackeray, C. Wolverton, E. D. Isaacs, *Energy Environ. Sci.* **2012**, *5*, 7854–7863.
- [11] V. Aravindan, J. Gnanaraj, Y.-S. Lee, S. Madhavi, *Chem. Rev.* **2014**, *114*, 11619–11635.
- [12] V. Aravindan, Y.-S. Lee, R. Yazami, S. Madhavi, *Mater. Today* **2015**, *18*, 345–351.
- [13] Q. Pan, F. Zheng, X. Ou, C. Yang, X. Xiong, M. Liu, *Chem. Eng. J.* **2017**, *316*, 393–400.

- [14] C. Yang, X. Ou, X. Xiong, F. Zheng, R. Hu, Y. Chen, M. Liu, K. Huang, *Energy Environ. Sci.* **2017**, *10*, 107–113.
- [15] A. Chaturvedi, P. Hu, V. Aravindan, C. Kloc, S. Madhavi, *J. Mater. Chem. A* **2017**, *5*, 9177–9181.
- [16] A. Chaturvedi, P. Hu, C. Kloc, Y.-S. Lee, V. Aravindan, S. Madhavi, *J. Mater. Chem. A* **2017**, *5*, 19819–19825.
- [17] Q. Pan, F. Zheng, Y. Wu, X. Ou, C. Yang, X. Xiong, M. Liu, *J. Mater. Chem. A* **2018**, *6*, 592–598.
- [18] O. Xing, Y. Chenghao, X. Xunhui, Z. Fenghua, P. Qichang, J. Chao, L. Meilin, H. Kevin, *Adv. Funct. Mater.* **2017**, *27*, 1606242.
- [19] V. Aravindan, Y. S. Lee, *Adv. Energy Mater.* **2018**, *8*, 1702841.
- [20] A. Chaturvedi, V. Aravindan, P. Hu, R. R. Prabhakar, L. H. Wong, C. Kloc, S. Madhavi, *Appl. Mater. Today* **2016**, *5*, 68–72.
- [21] A. Chaturvedi, E. Edison, N. Arun, P. Hu, C. Kloc, V. Aravindan, S. Madhavi, *ChemistrySelect* **2018**, *3*, 524–528.
- [22] B. G. Silbernagel, M. S. Whittingham, *Mater. Res. Bull.* **1976**, *11*, 29–36.
- [23] F. Croce, S. Passerini, B. Scrosati, E. Plichta, W. Behl, M. Salomon, D. Schleich, *J. Power Sources* **1993**, *44*, 481–484.
- [24] T. Stephenson, Z. Li, B. Olsen, D. Mitlin, *Energy Environ. Sci.* **2014**, *7*, 209–231.
- [25] C. H. Ho, Y. S. Huang, P. C. Liao, K. K. Tiong, *J. Phys. Chem. Solids* **1999**, *60*, 1797–1804.
- [26] B. Jariwala, D. Voiry, A. Jindal, B. A. Chalke, R. Bapat, A. Thamizhavel, M. Chhowalla, M. Deshmukh, A. Bhattacharya, *Chem. Mater.* **2016**, *28*, 3352–3359.
- [27] V. Aravindan, Y.-S. Lee, S. Madhavi, *Adv. Energy Mater.* **2017**, *7*, 1602607.
- [28] P. Poizot, S. Laruelle, S. Gruegeon, L. Dupont, J. M. Tarascon, *Nature* **2000**, *407*, 496–499.
- [29] H. Hwang, H. Kim, J. Cho, *Nano Lett.* **2011**, *11*, 4826–4830.
- [30] X. Fang, C. Hua, X. Guo, Y. Hu, Z. Wang, X. Gao, F. Wu, J. Wang, L. Chen, *Electrochim. Acta* **2012**, *81*, 155–160.
- [31] Q. Zhang, S. Tan, R. G. Mendes, Z. Sun, Y. Chen, X. Kong, Y. Xue, M. H. Rümmeli, X. Wu, S. Chen, L. Fu, *Adv. Mater.* **2016**, *28*, 2616–2623.
- [32] F. Qi, J. He, Y. Chen, B. Zheng, Q. Li, X. Wang, B. Yu, J. Lin, J. Zhou, P. Li, W. Zhang, Y. Li, *Chem. Eng. J.* **2017**, *315*, 10–17.
- [33] F. Qi, Y. Chen, B. Zheng, J. He, Q. Li, X. Wang, B. Yu, J. Lin, J. Zhou, P. Li, *J. Mater. Sci.* **2017**, *52*, 3622–3629.
- [34] F. Qi, Y. Chen, B. Zheng, J. He, Q. Li, X. Wang, J. Lin, J. Zhou, B. Yu, P. Li, W. Zhang, *Appl. Surf. Sci.* **2017**, *413*, 123–128.

Manuscript received: April 3, 2018
Version of record online: May 30, 2018